First European Conference on Earthquake Engineering and Seismology
(a joint event of the 13th ECEE & 30th General Assembly of the ESC)
Geneva, Switzerland, 3-8 September 2006
Paper Number: 458

NEXT GENERATION ATTENUATION (NGA) EMPIRICAL GROUND MOTION MODELS: CAN THEY BE USED IN EUROPE?

Kenneth W. CAMPBELL[1] and Yousef BOZORGNIA[2]

SUMMARY

We are one of five teams developing empirical ground motion models (attenuation relationships) for active shallow crustal regions as part of the PEER Next Generation Attenuation (NGA) Project. Each NGA Developer Team was provided with a common database of worldwide strong-motion recordings but used different data selection criteria, parameters, and functional forms in the development of their models. One of the biggest challenges was to develop a functional form that accounted for the apparent change in magnitude scaling around **M** 6.5–7.0 that was indicated by several recent large worldwide earthquakes. We selected a trilinear rather than the more traditional quadratic functional form for magnitude scaling to allow more flexibility in modeling magnitude-scaling effects between small and large earthquakes. Parameters included in the model are moment magnitude, closest distance to rupture, buried reverse faulting, normal faulting, sediment depth (both shallow and basin effects), hanging-wall effects, average shear-wave velocity in the top 30 m, and nonlinear soil response as a function of shear-wave velocity and rock PGA. A comparison of our NGA model with a recent attenuation relationship for Europe indicates that our model and likely the other NGA models can be used in this region. The largest discrepancies appear to be due to the use of linear magnitude scaling and linear site factors in the European model. More detailed evaluations will be needed to confirm this preliminary conclusion.

1. INTRODUCTION

In 2003, we and four other Developer Teams were selected to participate in a Pacific Earthquake Engineering Research Center (PEER) project to empirically develop Next Generation Attenuation (NGA) empirical ground motion models (EGMMs). Each Team used a common worldwide database of strong-motion recordings and supporting metadata that was developed by a sixth NGA team, but each Developer Team was allowed to apply its own selection criteria regarding which earthquakes, recordings, functional forms, and independent variables were to be used in developing its model. The NGA Project specified a set of minimum requirements that all models should meet, the most notable of which were that ground-motion predictions should be valid up to moment magnitude (**M**) 8.5 for strike-slip earthquakes, to **M** 8.0 for reverse-faulting earthquakes, to distances of 200 km, and to spectral periods of 10 s. A thorough description of the database development and project requirements are provided in several NGA project reports and summarized in a paper published in the proceedings of the Eighth U.S. National Conference on Earthquake Engineering [Power et al., 2006].

At the time this paper was written, our model had not yet been finalized. However, we do not expect that there will be significant changes to the preliminary results given in this paper. The functional forms are not likely to change significantly, but there are a few issues yet to be resolved that could require some minor adjustments of the model. Some of these issues were raised during an independent review and workshop held by the U.S.

[1] EQECAT Inc., 1030 NW 161st Place, Beaverton, Oregon 97006, USA
Email: kcampbell@eqecat.com
[2] Pacific Earthquake Engineering Research Center, 1301 S 46th Street, Bldg. 451, Richmond, California 94804, USA
Email: yousef@berkeley.edu

Geological Survey (USGS). Others are related to our ongoing development and tasks that need to be completed prior to publishing the final model. These issues include: (1) the use of worldwide versus western North American data, (2) the impact of surface versus buried rupture for strike-slip and normal-faulting earthquakes, (3) hanging-wall effects for normal-faulting earthquakes, (4) extrapolation of the model to a spectral period of 10 s, and (5) smoothing the regression coefficients.

2. STRONG-MOTION DATABASE

The NGA database includes strong-motion recordings generally intended to represent free-field conditions (e.g., large buildings were excluded). However, we applied additional criteria for deciding whether an earthquake or recording should be used. For example, an earthquake was used only if the following applied: (1) it occurred within the shallow continental lithosphere, (2) it was in a region considered to be tectonically active, (3) it had enough recordings to establish a reasonable earthquake source term, (4) it was a mainshock or triggered event and not an aftershock, and (5) it had generally reliable source parameters. A recording was used only if the following applied: (1) it was at or near ground level, (2) it had negligible soil-structure interaction effects, and (3) it had generally reliable site parameters.

An earthquake was considered to be poorly recorded and excluded from our database if it met the following criteria in terms of moment magnitude (**M**), number of recordings (N), and closest distance to rupture (R_{RUP}): (1) $\mathbf{M} < 5.0$ and $N < 5$, (2) $5.0 \leq \mathbf{M} < 6.0$ and $N < 3$, and (3) $6.0 \leq \mathbf{M} < 7.0$, all recordings have $R_{RUP} > 60$ km and $N < 2$. Note that singly recorded earthquakes with $\mathbf{M} \geq 7$ and $R_{RUP} \leq 60$ km were retained because of their importance in constraining near-source ground motions in large earthquakes. Specific details regarding how these general criteria were implemented to select the recordings and metadata used in the regression analysis will be documented in a PEER report at the end of the project. The selected database includes 1561 three-component recordings from 64 worldwide earthquakes with $\mathbf{M} = 4.2$–7.9 and $R_{RUP} = 0$–200 km (Figure 1).

3. REGRESSION ANALYSES

During the exploratory (model building) phase of the study, regression analyses were performed for a selected number of spectral periods in two stages, using the two-step regression procedure described by Boore et al. [1993] except that each step used nonlinear rather than linear regression. In Stage 1, all of those functions involving individual recordings (intra-event terms) were fit by the method of nonlinear least squares, in which each earthquake was constrained to have a zero mean residual by assigning it an earthquake source term. These functions included Equation 3 and Equations 6–11 in the model presented in the next section. In Stage 2, all of those functions involving the earthquake source terms from Stage 1 (inter-event terms) were fit using the method of weighted nonlinear least squares, where each source term was assigned a weight that was inversely proportional to its variance in Stage 1. These functions included Equation 2 and Equations 4–5 in the model presented in the next section. This two-step analysis allowed us to decouple the intra-event terms from the inter-event terms, which made the regression analyses relatively stable and allowed us to independently evaluate and model ground-motion scaling effects at large magnitudes. Once the functional forms and model parameters were selected, we used random effects regression [Abrahamson and Youngs, 1992] to derive the final model coefficients for all spectral periods.

4. GROUND MOTION MODEL

We developed the functional forms for the independent variables used in the empirical ground motion model (EGMM) from classical data exploration techniques, such as analysis of residuals. Candidate functional forms were developed through numerous iterations to capture the observed trends in the recorded ground-motion data. The final forms included mathematical expressions developed by ourselves, taken from the literature, derived from theoretical studies, and proposed by the other NGA Developer Teams during a series of interaction meetings. We selected the final functional forms based on the following criteria: (1) their simplicity, although this was not an overriding factor, (2) their seismological bases, (3) their unbiased residuals, and (4) their ability to be extrapolated to parameter values important to engineering applications, especially probabilistic seismic hazard analysis (PSHA). Criterion 4 was the most difficult to meet, because the data did not always allow the functional forms to be developed empirically. In such cases, theoretical constraints were used to define these functional forms based on supporting studies conducted as part of the NGA Project [Power et al., 2006].

The general functional form of the our EGMM is given by the equation

$$\ln Y = f_1(\mathrm{M}) + f_2(\mathrm{R}) + f_3(\mathrm{F}) + f_4(\mathrm{HW}) + f_5(\mathrm{S}) + f_6(\mathrm{D}) + \varepsilon_T \tag{1}$$

where f_i are functions of magnitude (M), source-to-site distance (R), style of faulting (F), hanging-wall effects (HW), shallow site conditions (S), and sediment depth (D).

The dependence on magnitude is modeled by

$$f_1(\mathrm{M}) = \begin{cases} c_0 + c_1\mathbf{M} & \mathbf{M} \le 5.5 \\ c_0 + c_1\mathbf{M} + c_2(\mathbf{M} - 5.5) & 5.5 < \mathbf{M} \le 6.5 \\ c_0 + c_1\mathbf{M} + c_2(\mathbf{M} - 5.5) + c_3(\mathbf{M} - 6.5) & \mathbf{M} > 6.5 \end{cases} \tag{2}$$

The dependence on source-to-site distance is modeled by

$$f_2(\mathrm{R}) = (c_4 + c_5\mathbf{M})\ln\left(\sqrt{R_{RUP}^2 + c_6^2}\right) \tag{3}$$

The dependence on style of faulting is modeled by

$$f_3(\mathrm{F}) = c_7 F_{RV}\, f_{\mathrm{F}}(Z_{TOR}) + c_8 F_{NM} \tag{4}$$

where

$$f_{\mathrm{F}}(Z_{TOR}) = \begin{cases} Z_{TOR} & Z_{TOR} < 1 \\ 1 & Z_{TOR} \ge 1 \end{cases} \tag{5}$$

The dependence on hanging-wall effects is modeled by

$$f_4(\mathrm{HW}) = c_9 F_{RV}\, f_{\mathrm{HW}}(R_{RUP}, R_{JB})\, f_{\mathrm{HW}}(\mathrm{M})\, f_{\mathrm{HW}}(Z_{TOR}) \tag{6}$$

where

$$f_{\mathrm{HW}}(R_{RUP}, R_{JB}) = \begin{cases} 1 & R_{JB} = 0 \\ (R_{RUP} - R_{JB}) / R_{RUP} & R_{JB} > 0 \end{cases} \tag{7}$$

$$f_{\mathrm{HW}}(\mathrm{M}) = \begin{cases} 0 & \mathbf{M} \le 6.0 \\ 2(\mathbf{M} - 6.0) & 6.0 < \mathbf{M} < 6.5 \\ 1 & \mathbf{M} \ge 6.5 \end{cases} \tag{8}$$

$$f_{\mathrm{HW}}(Z_{TOR}) = \begin{cases} 0 & Z_{TOR} \ge 20 \\ (20 - Z_{TOR}) / 20 & Z_{TOR} < 20 \end{cases} \tag{9}$$

The dependence on shallow site conditions (both linear and nonlinear) is modeled by

$$f_5(\mathrm{S}) = \begin{cases} c_{10}\ln\left(\dfrac{V_{S30}}{k_1}\right) + k_2\left\{\ln\left[A_{1100} + c\left(\dfrac{V_{S30}}{k_1}\right)^n\right] - \ln\left[A_{1100} + c\right]\right\} & V_{S30} < k_1 \\ (c_{10} + k_2 n)\ln\left(\dfrac{V_{S30}}{k_1}\right) & V_{S30} \geq k_1 \end{cases} \tag{10}$$

The dependence on sediment depth (both shallow and 3-D basin effects) are modeled by

$$f_6(\mathrm{D}) = \begin{cases} c_{11}(Z_{2.5} - 1) & Z_{2.5} < 1 \\ 0 & 1 \leq Z_{2.5} \leq 3 \\ c_{12}k_3\left[e^{-0.75} - e^{-0.75(Z_{2.5}/3)}\right] & Z_{2.5} > 3 \end{cases} \tag{11}$$

In the above equations, Y is the geometric mean of the two horizontal components of the peak ground acceleration (PGA) or the 5%-damped pseudo-absolute acceleration response spectral ordinate (SA) in g; **M** is moment magnitude; R_{RUP} is closest distance to coseismic rupture in kilometers; R_{JB} is closest distance to the surface projection of coseismic rupture (Joyner-Boore distance) in kilometers; F_{RV} is an indicator variable representing reverse (including reverse-oblique) faulting, where F_{RV} = 1 for 30° < λ < 150° and F_{RV} = 0 otherwise and λ is rake angle, defined as the average angle of slip in degrees measured in the plane of rupture between the strike direction and the slip vector; F_{NM} is an indicator variable representing normal (including normal-oblique) faulting, where F_{NM} = 1 for –150° < λ < –30° and F_{NM} = 0 otherwise; Z_{TOR} is depth to the top of coseismic rupture in kilometers; V_{S30} is average shear-wave velocity in the top 30 m of the site profile in meters per second; A_{1100} is the value of PGA on a rock site with V_{S30} = 1100 m/s; $Z_{2.5}$ is depth to the 2.5 km/s shear-wave velocity horizon (hereafter referred to as sediment depth) in kilometers; n and c are period-independent, theoretically constrained model coefficients; k_i are period-dependent, theoretically constrained model coefficients; c_i are empirically derived model coefficients; and ε_T is a random error term with a mean of zero and a total aleatory standard deviation given by

$$\sigma_T = \sqrt{\sigma^2 + \tau^2} \tag{12}$$

where σ is the standard deviation of the intra-event residuals and τ is the standard deviation of the inter-event residuals. It is interesting to note that these standard deviations were not found to be a significant function of magnitude as has been found in past studies. The larger number of high-quality intra-event recordings for both small- and large-magnitude earthquakes suggests that the previously observed strong dependence of aleatory uncertainty on magnitude by Campbell and Bozorgnia [2003] and other researchers was largely an artifact of poorly recorded events at the upper and lower magnitude limits of the data. The large number of events and recordings in the present study has allowed us to adopt more restrictive selection criteria, especially with respect to the minimum number of recordings for small-magnitude earthquakes, which has significantly improved the analysis and reduced the inter-event variability of these smaller events. The increase in the number of well-recorded earthquakes at large magnitudes has resulted in a better, albeit increased, estimate of intra-event variability for these larger events. It is possible that we might find some weak dependence on magnitude or even a dependence on ground-motion amplitude before the study is completed.

We have found the aleatory standard deviation to depend on the level of ground shaking for the softer sites. This is due to the correlation between rock PGA (A_{1100}) and ground-motion amplitude inherent in Equation (10), especially for sites with low values of V_{S30}, which we generically refer to as soil. As rock PGA increases, the nonlinear behavior of soil tends to decrease its amplification effects. On the other hand, as rock PGA decreases, the more linear behavior of the soil tends to increase its amplification effects. This self-compensating behavior reduces the variability of PGA and SA on soil compared to that on rock. These effects are minimal for $V_{S30} \geq 760$ m/s (NEHRP site categories A and B), but they become significant for $V_{S30} \leq 360$ m/s (NEHRP site categories D and E). A definition of NEHRP site categories in terms of V_{S30} can be found in BSSC [2004]. We are currently in the process of developing a marginal aleatory uncertainty model for soil sites as a function of V_{S30}.

4.1 Considerations in the Selection of Functional Forms

4.1.1 Magnitude Term

The trilinear magnitude-scaling term in Equation 2 was derived from both an analysis of residuals and theoretical considerations. It models the observed decrease in the amount of magnitude scaling above **M** 6.5 that was identified in the Stage 2 regression analysis. This behavior, which had been noted in previous studies but not considered to be credible, became very evident in some well-recorded recent large-magnitude earthquakes in Alaska, California, Turkey and Taiwan. In fact, the regression analysis was producing a slight tendency for over-saturation of short-period ground motion at large magnitudes and short distances. Although some seismologists believe that such over-saturation in short-period ground motion is possible for very large earthquakes, we did not find this behavior to be statistically significant. Therefore, we constrained the coefficient c_3 in Equation 2 to prevent over-saturation. Other functional forms were either found to be too difficult to constrain empirically, such as the hyperbolic tangent function of Campbell [1997] or the magnitude-dependent pseudo-distance term used by Campbell and Bozorgnia [2003], or could not be reliably extrapolated to magnitudes as large as **M** 8.5 as required by the NGA Project, such as the quadratic function used by Boore et al. [1997]. For example, in our previous model [Campbell and Bozorgnia, 2003], we forced magnitude saturation at all spectral periods in order to prevent over-saturation as well as to stabilize the nonlinear regression analysis.

4.1.2 Distance Term

The distance-scaling term in Equation 3 is similar to that used by Abrahamson and Silva [1997]. Our previous model [Campbell and Bozorgnia, 2003], which was developed for distances of 60 km and less but often used at larger distances, assumed a constant rate of attenuation with magnitude. Since the NGA Project required that the EGMM be valid to distances of 200 km, we found it was important to include magnitude-dependent distance scaling in our model in order to extend it to such large distances. The magnitude-dependent distance scaling predicted by Equation 3 approximates the effects of anelastic attenuation, which Campbell [1997] found to be magnitude-dependent, at least out to the maximum distance of 200 km required by the NGA Project,.

4.1.3 Style-of-Faulting Term

The style-of-faulting term in Equations 4 and 5 was derived from an analysis of residuals. It introduces a new parameter, depth to the top of coseismic rupture (Z_{TOR}), that indicates whether or not coseismic rupture extends to the surface. This new parameter was found to be most significant at short periods for reverse faulting, although its impact on other types of faulting is still being evaluated. Ground motion was found to be significantly higher for reverse faulting when rupture did not break to the surface (i.e., when $Z_{TOR} > 1.0$ km), no matter whether this rupture was on a blind thrust or on a fault with historical or paleoseismic surface rupture. When rupture broke to the surface, the ground motion for reverse faulting was found to be comparable to that for strike-slip faulting. This effect is linearly decreased to zero from a depth of 1.0 to 0 km to provide a smooth transition from buried to surface faulting. This transition depth is somewhat arbitrary and was selected so that those faults assigned a depth to the top of rupture of 1.0 km in the 2002 U.S. national seismic hazard source model would be treated as a buried fault. Some strike-slip earthquakes with partial or weak surface expression also appeared to have higher-than-average ground motion (e.g., 1995 Kobe, Japan), but additional studies will be required to determine if this is predictable. The coefficient for normal faulting was found to be only marginally significant at short periods. It has been retained at this time because of its potential significance at longer periods.

4.1.4 Hanging-Wall Term

Like the style-of-faulting term, the hanging-wall term in Equations 6–9 was derived from an analysis of residuals. The functional form for Equation 7, the term that involves both R_{RUP} and R_{JB}, was suggested by the Chiou-Youngs NGA Developer Team. We had first proposed a somewhat more complicated functional form that had similar behavior for surface-rupturing earthquakes. However, we switched to the Chiou-Youngs functional form because of its added advantage of smearing out hanging-wall effects over the top edge of a buried rupture, which has been suggested from observations of overturned rocks and transformers near the White Wolf Fault, source of the 1952 Kern County earthquake, by Brune et al. [2004]. We included Equations 8 and 9 to phase out hanging-wall effects at small magnitudes and large depths, where the residuals suggest that the effects are negligible or are not resolvable from the data. As the functional form is defined now, the hanging-wall effects end abruptly at the fault trace of a surface-rupturing earthquake. We believe that there should be a smooth transition in hanging-wall effects from the hanging-wall to the footwall for such a rupture and are looking into a means of incorporating this effect in Equation 7.

4.1.5 Shallow Site-Conditions Term

The linear part of the shallow site-conditions term ($V_{s30} \geq k_1$) in Equation 10 is similar to that adopted by Boore et al. [1997]. The nonlinear part of this term ($V_{s30} < k_1$) was constrained from theoretical studies conducted as part of the NGA Project [Walling and Abrahamson, 2006], since the empirical data were insufficient to constrain the complex nonlinear behavior of the softer soils. After including a linear site term, the resulting residuals clearly indicated the presence of nonlinear behavior of PGA and SA at short periods, but these residuals when plotted against rock PGA (A_{1100}) could not be used to determine how this complex behavior varied with V_{S30}, A_{1100} and spectral period. The linear behavior of this model was determined from regression analysis after constraining the nonlinear term to that proposed by Walling and Abrahamson [2006]. These authors developed two sets of nonlinear model coefficients based on equivalent-linear site-response calculations conducted as part of the NGA Project [Silva, 2005]. We chose to use the coefficients based on the more linear strain-dependent shear modulus reduction and damping curves (the so-called PEN model) after Walt Silva [personal communication, 2005] suggested that they were probably appropriate for a broader class of sites. We also found that our intra-event standard deviation was slightly lower when we used these coefficients, although the difference was not statistically significant.

4.1.6 Sediment-Depth Term

The sediment-depth term in Equation 11 has two parts: (1) a term to model 3-D basin effects for $Z_{2.5} > 3.0$ km and (2) a term to model the effects of shallow sediments for $Z_{2.5} < 1.0$ km, both of which are significant only at longer spectral periods. We modeled the depth and period dependence of the basin-effects term with a theoretical model developed as part of the NGA Project [Day et al., 2006] from 3-D ground-motion simulations that included the response of the Los Angeles, San Gabriel, and San Fernando Basins in southern California. At our request, Steve Day [written communication, 2005] extended this model to include the depth to the 2.5 km/s shear-wave velocity horizon. After including the shallow site conditions term in Equation 10, the resulting residuals clearly indicated a strong positive trend with $Z_{2.5}$ and spectral period for $Z_{2.5} > 3.0$ km, similar to that found by Day et al. [2006]. However, unlike these authors who found that ground motion was strongly correlated with $Z_{2.5}$ between depths of 1.0 and 3.0 km, we did not find any trend in our residuals in this depth range. This effect is apparently accounted for by other parameters in our model (most likely V_{S30}). We calibrated the theoretical basin-effects model by including an empirical coefficient. We also eliminated the first term of the theoretical model because we only applied it at large depths. We believe that the observed decrease in long-period ground motion at shallow sediment depths ($Z_{2.5} < 1.0$ km) might be a result of the sediment cover being too thin to fully amplify this motion. Thus, this term likely compensates for a potential over-amplification of ground motion predicted by the shallow site-conditions term in Equation 10, which is dominated by recordings on deeper sites.

5. APPLICABILITY TO EUROPE

Although we have always included worldwide earthquakes from tectonically active shallow crustal regions in the development of our EGMMs, the same cannot be said for the previous models of the other NGA Developer Teams. This attitude changed during the course of the NGA Project, where all of the Developer Teams decided to include worldwide earthquakes in the development of their models. As a result, it is likely that these models can be used in regions other than that for which they were originally intended (i.e., the Western United States). To test whether these models might be appropriate for use in the tectonically active shallow crustal regions of Europe, we have compared predictions from our EGMM with those from a recently published EGMM for Europe and the Middle East developed by Ambraseys et al. [2005].

The Ambraseys et al. functional form is given by the following equation:

$$\log Y = a_1 + a_2 M_W + (a_3 + a_4 M_W)\log\left(\sqrt{d^2 + a_5^2}\right) + a_6 S_S + a_7 S_A + a_8 F_N + a_9 F_T + a_{10} F_O \tag{13}$$

where M_W is moment magnitude, d is Joyner-Boore distance in kilometers, S_S = 1 for soft soil sites and 0 otherwise, S_A = 1 for stiff soil sites and 0 otherwise, F_N = 1 for normal-faulting earthquakes and 0 otherwise, F_T = 1 for thrust-faulting (i.e., reverse-faulting) earthquakes and 0 otherwise, and F_O = 1 for odd-faulting earthquakes and 0 otherwise. We have used Ambraseys et al. original symbols for traceability, but many of these parameters are the same or similar to those used in our EGMM. For example, their M_W is equivalent to our **M**, their d is equivalent to our R_{JB}, their F_N is equivalent to our F_{NM}, and their F_T is equivalent to our F_{RV}.

The Ambraseys et al. EGMM uses site categories rather than V_{S30} to model site effects. However, like the NEHRP site categories, their categories are defined in terms of a range of V_{S30} values. Based on the ranges of V_{S30} that these authors used to define their site categories, we find their soft-soil category to be equivalent to NEHRP D, their stiff-soil category to be equivalent to NEHRP C, and their rock category (i.e., $S_S = S_A = 0$) to be equivalent to NEHRP B. We have evaluated our EGMM for V_{S30} = 270 m/s (the midpoint of NEHRP D) to compare with their soft soil, for V_{S30} = 560 m/s (the midpoint of NEHRP C) to compare with their stiff soil, and for V_{S30} = 1130 m/s (the midpoint of NEHRP B) to compare with their rock. A better comparison could have been achieved if we could have evaluated our EGMM for the mean V_{S30} for each of their site categories, but this value was not given. All comparisons are for strike-slip faulting.

Because of length limitations, we cannot show all of the comparisons we made. Instead, we provide a representative sample of these comparisons for PGA and SA(1.0s). Magnitude-scaling effects are compared in Figure 2 for NEHRP B, C and D site conditions; site factors are compared in Figure 3; distance-scaling effects are compared in Figure 4 for NEHRP B, C and D site conditions; and total aleatory standard deviations (natural log) are compared in Figure 5.

Although a quick look at the comparisons would appear to indicate that the two sets of predictions are very different, a closer look indicates that they are generally comparable over the range of magnitudes and distances where the Ambraseys et al. model is well constrained (M = 5.0–6.5 and R_{JB} = 10–100 km for strike-slip faulting). For example, the comparison for NEHRP B site conditions in Figures 2a, 2b, 4a and 4b, where nonlinear soil behavior is negligible, show generally good agreement in this data range. The greatest differences are at small distances and large magnitudes, where our model predicts significant nonlinear magnitude-scaling, and at large distances, where our model predicts slightly less attenuation. Figures 2c, 2d, 4c and 4d indicate that this agreement worsens somewhat for NEHRP D site conditions. The reason for this can be seen in Figure 3, where the nonlinear soil behavior predicted by our model results in larger site factors (site amplification) at lower values of rock PGA and lower site factors at higher values of rock PGA. A comparison of standard deviations in Figure 5 shows that our aleatory uncertainty is considerably smaller than that predicted by the Ambraseys et al. model. The magnitude dependence predicted by their PGA model, although it is consistent with our previous model, might result from the same data selection issues discussed above.

6. CONCLUSIONS

Thanks to the NGA Project, we believe that our new empirical ground motion model (EGMM) represents a quantum jump in our ability to predict ground motions over a wide range of seismological and site parameters. The large number of these parameters that were made available through the NGA Project has also allowed us to better quantify source, propagation, and site effects as well as to add new parameters to our EGMM to make it a more useful engineering tool. A comparison of our NGA EGMM with a similar recent model developed for Europe and the Middle East by Ambraseys et al. [2005] suggests that our, and by analogy the other, NGA models can possibly be used in the tectonically active shallow crustal regions of Europe. The largest discrepancies are caused by our nonlinear versus their linear magnitude scaling and our nonlinear versus their linear site factors. A better test would be to look for a significant bias in the residuals of the European strong-motion dataset with respect to our EGMM, which we hope to do in a future study.

7. REFERENCES

Abrahamson, N.A. and Silva, W.J. (1997), Empirical Response Spectral Attenuation Relations for Shallow Crustal Earthquakes, *Seismological Research Letters*, 68, 94–127.

Abrahamson, N.A. and Youngs, R.R. (1992), A Stable Algorithm for Regression Analyses Using the Random Effects Model, *Bulletin of the Seismological Society of America*, 82, 505–510.

Ambraseys, N.N., Douglas, J., Sarma, S.K. and Smit, P.M. (2005), Equations for the Estimation of Strong Ground Motions from Shallow Crustal Earthquakes Using Data from Europe and the Middle East: Horizontal Peak Ground Acceleration and Spectral Acceleration, *Bulletin of Earthquake Engineering*, 3, 1–53.

Boore, D.M., Joyner, W.B. and Fumal, T.E. (1993), Estimation of Response Spectra and Peak Accelerations from Western North American Earthquakes: An Interim Report, *U.S. Geological Survey Open-File Report 93-509*.

Boore, D.M., Joyner, W.B. and Fumal, T.E. (1997), Equations for Estimating Horizontal Response Spectra and Peak Acceleration from Western North American Earthquakes: A Summary of Recent Work, *Seismological Research Letters*, 68, 128–153.

Brune, J.N., Anooshehpoor, A., Shi, B. and Zeng, Y. (2004) Precarious Rock and Overturned Transformer Evidence for Ground Shaking in the M_s 7.7 Kern County Earthquake: An Analog for Disastrous Shaking from a Major Thrust Fault in The Los Angeles Basin, *Bulletin of the Seismological Society of America*, 94, 1993–2003.

BSSC (2004), NEHRP (National Earthquake Hazard Reduction Program) Recommended Provisions for New Buildings and Other Structures (FEMA 450), 2003 Edition, *Building Seismic Safety Council, National Institute of Building Sciences*, Washington, D.C.

Campbell, K.W. (1997), Empirical Near-Source Attenuation Relationships for Horizontal and Vertical Components of Peak Ground Acceleration, Peak Ground Velocity, and Pseudo-Absolute Acceleration Response Spectra, *Seismological Research Letters*, 68, 154–179.

Campbell, K.W., and Bozorgnia, Y. (2003), Updated Near-Source Ground Motion (Attenuation) Relations for the Horizontal and Vertical Components of Peak Ground Acceleration and Acceleration Response Spectra, *Bulletin of the Seismological Society of America*, 93, 314–331.

Day, S.M., Bielak, J., Dreger, D., Graves, R., Larsen, S., Olsen, K.B., Pitarka, A. and Ramirez-Guzman, L. (2006), Numerical Simulation of Basin Effects on Long-Period Ground Motion, *Proceedings of the 8th U.S. National Conference on Earthquake Engineering, Paper No. 1857*.

Power, M., Chiou, B., Abrahamson, N. and Roblee, C. (2006), The "Next Generation of Ground Motion Attenuation Models" (NGA) Project: An Overview, *Proceedings of the 8th U.S. National Conference on Earthquake Engineering, Paper No. 2022*.

Silva, W.J. (2005), Site Response Simulations for the NGA Project, *Pacific Earthquake Engineering Research Center, draft report*, Richmond, California.

Walling, M. and Abrahamson, N. (2006) Non-linear Soil Response Model, *Proceedings of the 8th U.S. National Conference on Earthquake Engineering, Paper No. 1030*.

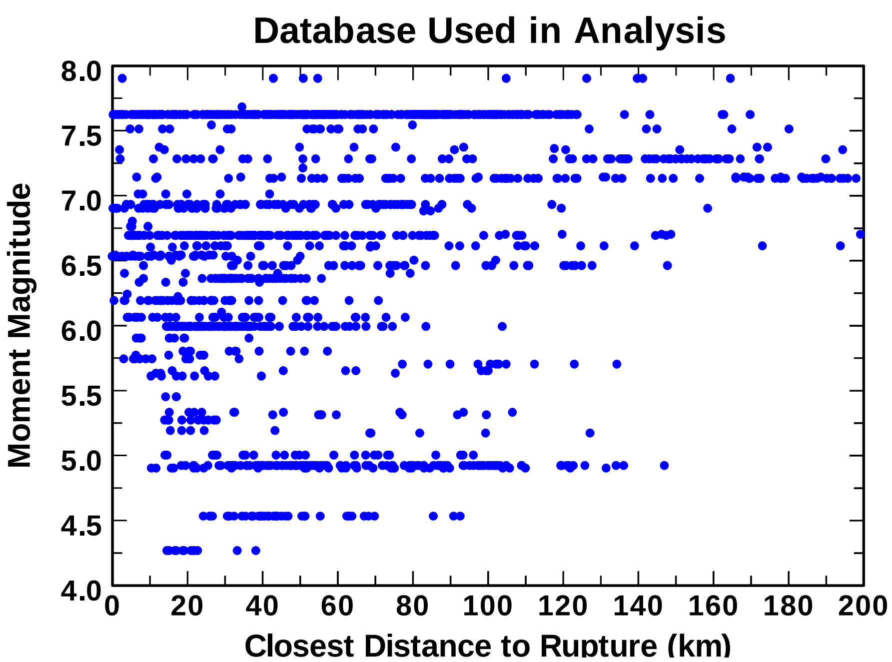

Figure 1: Database used in the development of the NGA empirical ground motion model.

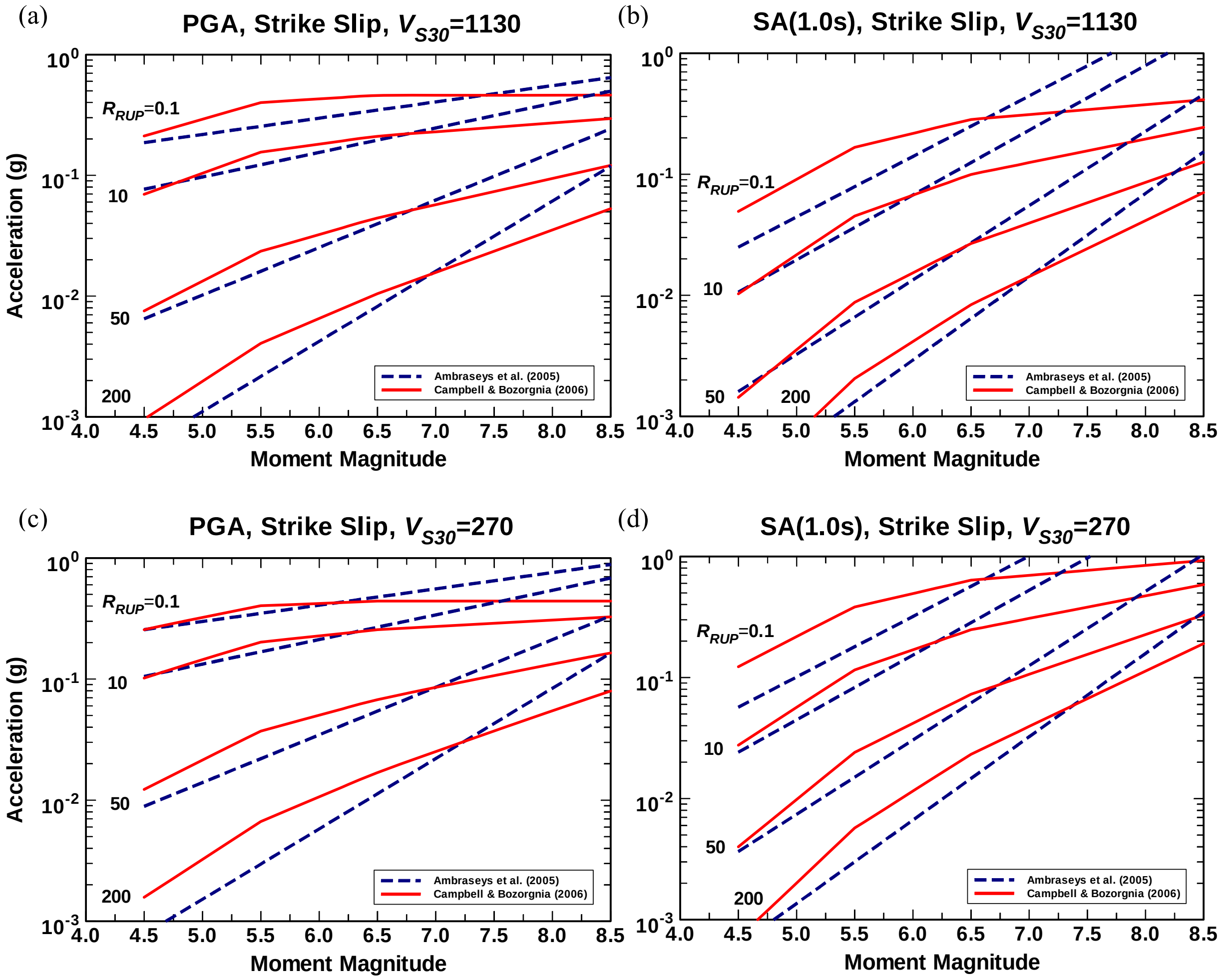

Figure 2: Comparison of magnitude-scaling characteristics predicted by the NGA and Ambraseys et al. (2005) empirical ground motion models: (a) PGA and NEHRP B site conditions, (b) SA(1.0s) and NEHRP B site conditions, (c) PGA and NEHRP D site conditions, (d) SA(1.0s) and NEHRP D site conditions.

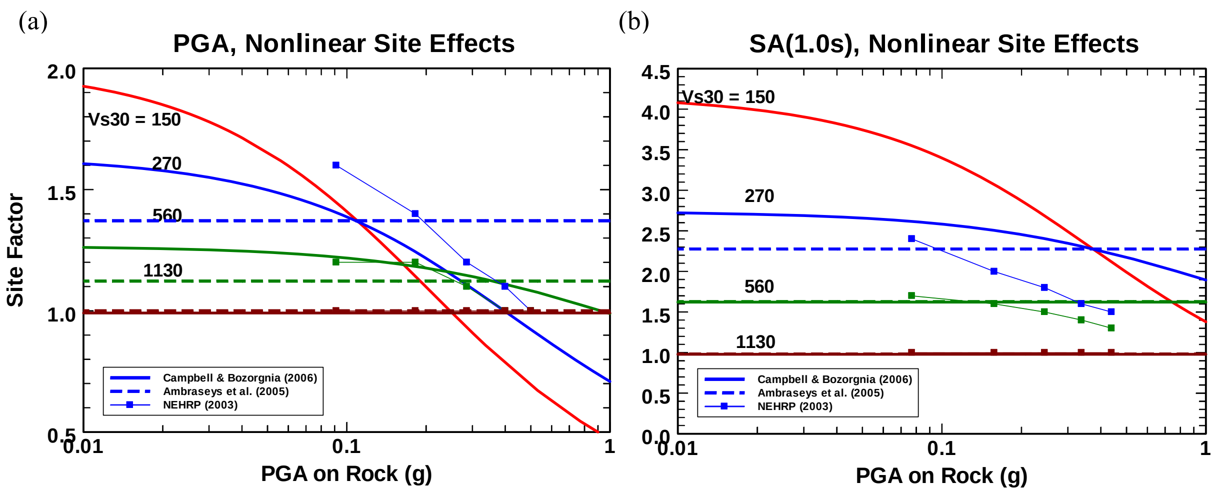

Figure 3: Comparison of site factors predicted by the NGA and Ambraseys et al. (2005) empirical ground motion models and by the NEHRP provisions: (a) PGA, (b) SA(1.0s).

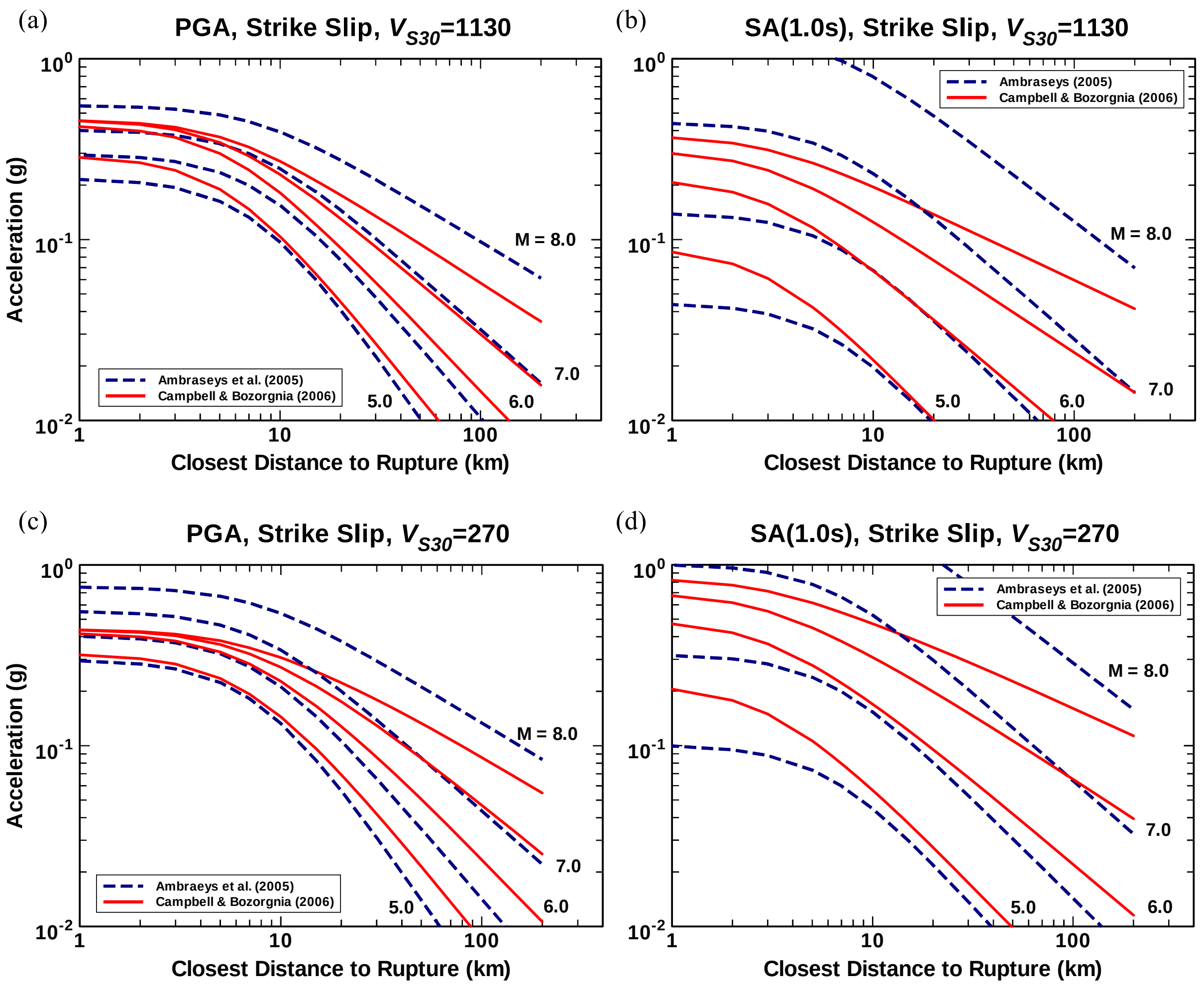

Figure 4: Comparison of distance-scaling characteristics predicted by the NGA and Ambraseys et al. (2005) empirical ground motion models: (a) PGA and NEHRP B site conditions, (b) SA(1.0s) and NEHRP B site conditions, (c) PGA and NEHRP D site conditions, (d) SA(1.0s) and NEHRP D site conditions.

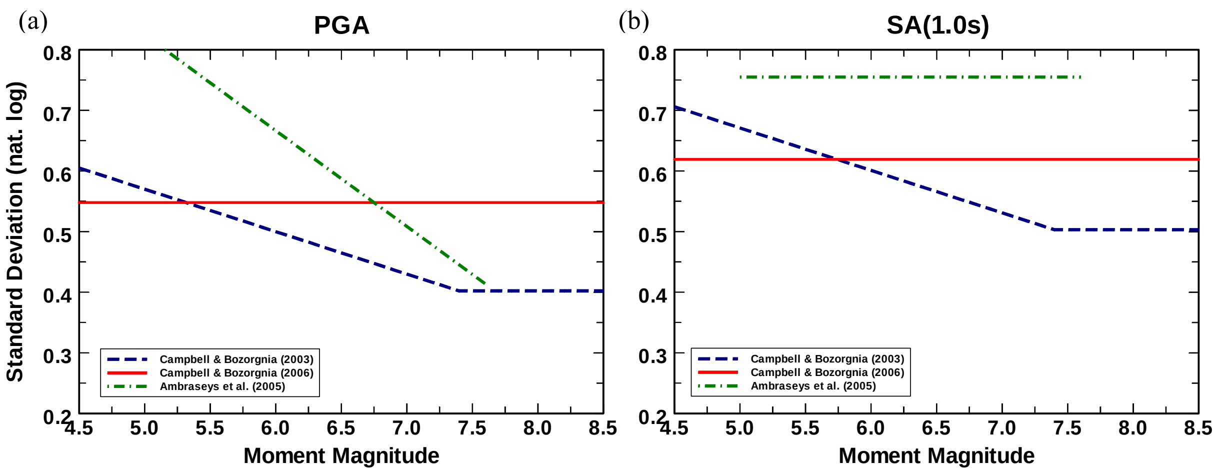

Figure 5: Comparison of aleatory standard deviations (natural log) predicted by the Campbell and Bozorgnia (NGA), Campbell and Bozorgnia (2003), and Ambraseys et al. (2005) empirical ground motion models.